Amplification of ENSO effects on Indian summer monsoon by absorbing aerosols

Maeng-Ki Kim[1], William K. M. Lau[2], Kyu-Myong Kim[3], Jeong Sang[1], Yeon-Hee Kim[4], and Woo-Seop Lee[5]

[1]Department of Atmospheric Science, Kongju National University, Gongju, 314-701, Korea

[2]Earth System Science Interdisciplinary Center, U. of Maryland, College Park, MD 20742, USA

[3]Laboratory for Atmospheres, NASA Goddard Space Flight Center, Greenbelt, MD 20771, USA

[4]School of Environmental Science and Engineering, Pohang University of Science and Technology (POSTECH), Pohang, Gyeongbuk, 790-784, Korea

[5]APEC Climate Center, Busan, 612-020, Korea

June 16, 2015

Climate Dynamics

Corresponding author: Maeng-Ki Kim, Dept. of Atmospheric Science, Kongju National University, Gongju, 314-701, Korea
Tel: +82-41-850-8531
Fax:+82-41-856-8527
Email: mkkim@kongju.ac.kr

Abstract

In this study, we present observational evidence, based on satellite aerosol measurements and MERRA reanalysis data for the period 1979-2011, indicating that absorbing aerosols can have strong influence on seasonal-to-interannual variability of the Indian summer monsoon rainfall, including amplification of ENSO effects. We find a significant correlation between ENSO (El Nino Southern Oscillation) and aerosol loading in April-May, with La Nina (El Nino) conditions favoring increased (decreased) aerosol accumulation over northern India, with maximum aerosol optical depth (AOD) over the Arabian Sea and Northwestern India, indicative of strong concentration of dust aerosols transported from West Asia and Middle East deserts. Composite analyses based on a normalized aerosol index (NAI) show that high concentration of aerosol over northern India in April-May is associated with increased moisture transport, enhanced dynamically induced warming of the upper troposphere over the Tibetan Plateau, and enhanced rainfall over northern India and the Himalayan foothills during May-June, followed by a subsequent suppressed monsoon rainfall over all India, consistent with the Elevated Heat Pump (EHP) hypothesis (Lau et al. 2006). Further analyses from sub-sampling of ENSO years, with normal (<1-σ), and abnormal (>1-σ)) NAI over northern India respectively show that the EHP may lead to an amplification of the Indian summer monsoon response to ENSO forcing, particularly with respect to the increased rainfall over the Himalayan foothills, and the warming of the upper troposphere over the Tibetan Plateau. Our results suggest that absorbing aerosol, particular desert dusts can strongly modulate ENSO influence, and possibly play important roles as a feedback agent in climate change in Asian monsoon regions. .

Keywords: EHP, monsoon, ENSO, absorbing aerosol, dust, black carbon

1. Introduction

Atmospheric aerosols, clouds and precipitation are key building blocks of the energy and water cycles of the earth's climate system (Haywood and Boucher 2000; Ramanathan et al. 2001; Bellouin et al. 2005; Wang 2013). Recently, an increasing body of studies have shown that absorbing aerosols such as black carbon and dust, most abundant in monsoon regions, play an important role in the radiation energy balance of the atmosphere and at the earth surface, with profound impact on the large scale circulation and rainfall in monsoon regions (Jacobson 2001; Chung et al. 2002; Menon et al. 2002; Ramanathan et al. 2005; Chung and Ramanathan 2006; Lau et al. 2006; Lau and Kim 2006; Kim et al. 2006; Kerr 2007; Bollasina et al. 2008; Lau et al. 2009; Meehl et al. 2008; Randles and Ramaswamy 2008; Collier and Zhang 2009; Wang et al. 2009a; Bollasina and Nigam 2011; Bollasina et al. 2011; Manoj et al. 2011; Cowan and Cai 2011; Ganguly et al. 2012; Bollasina et al. 2013, Vinoj et al. 2014; Lau 2014).

Specifically for the Indian monsoon, Ramanathan et al. (2005) showed that reduction in surface solar radiation, due to the absorption and scattering of incident solar radiation by aerosols, i.e., the solar dimming (SDM) effect, cools the northern Indian Ocean, reduces evaporation and meridional sea surface temperature gradient, resulting in a weakening of the local Hadley cell circulation, and reduction of the Indian summer monsoon precipitation. Lau et al. (2006) proposed the Elevated Heat Pump (EHP) effect, *i.e.*, atmospheric heating by absorbing aerosols (dust and black carbon) over northern India during the pre- and early monsoon season induces atmospheric feedback processes leading to increased monsoon rainfall and earlier onset of monsoon rain over northern India and the Himalayan foothills. Since the Lau et al. (2006) study, a number of modeling studies reported findings that are generally consistent, albeit varied in details, with the EHP, i.e., absorbing aerosols can increase rainfall in the early monsoon (April-June) over India. Meehl et al. (2008) showed further that the earlier monsoon rainfall increase due to black carbon aerosol heating could lead subsequently to a weakening of peak monsoon, through cloud and land surface feedback processes. Using a three-dimensional aerosol climate model based on the Community Climate Model version 3 (CAM3) of the National

Center of Atmospheric Research (NCAR), Wang et al. (2009b) showed that absorbing anthropogenic aerosols could shift convective precipitation northward over the Indian subcontinent, particularly during the onset season, via an increase in moist static energy in the sub-cloud layer. Using the NCAR Community Atmosphere Model CAM3, Collier and Zhang (2009) found that tropospheric shortwave heating over central India due to absorbing aerosols could increase convective instability during the pre-monsoon season (March to May), enhancing deep convection and rainfall, but suppress rainfall during the subsequent June-July period. Randles and Ramaswamy (2008) showed that an enhanced monsoon circulation associated with increased absorbing aerosol optical depth (AOD) results in increases of low-level convergence, upward motion, atmospheric water vapor, low-level cloud amount, and precipitation (particularly evident and statistically significant in the high optical depth regime), indicating that the increase of low level convergence and in upward motion overcome the stabilizing effects of absorbing aerosols resulting in enhanced monsoon circulation and precipitation in northwestern India. Furthermore, Ganguly et al. (2012) investigated the time-scale dependent responses of the South Asian monsoon to anthropogenic aerosol forcing using the Community Atmosphere Model (CAM5) with a fully predictive aerosol life cycle. They demonstrated that the slow response associated with sea surface temperature (SST) changes is generally stronger than the fast atmospheric response. However over the northern India (>25^{o} N), the fast response could be more important. Ganguly et al. (2012) also emphasized that both the SDM and EHP effects as well as the microphysical aerosol effect are important for altering the Indian monsoon. Using the Geophysical Fluid Dynamic Laboratory (GFDL) climate model with fully interactive aerosols and chemistry, Bollasina et al. (2013) showed that an earlier onset of the Indian summer monsoon has been induced by the direct global aerosol effect during the second half of the 20th century, emphasizing the importance of dynamic feedbacks and regional land-surface processes in aerosol-monsoon interactions. More recently, using satellite data and the Community Atmosphere Model (CAM5) model, Vinoj et al. (2014) found that heating of the atmosphere by dust aerosols over the Arabian Sea, transported from West Asia, and Arabian Peninsula may increase the influx of water vapor into India, inducing large-scale convergence and enhance

monsoon rainfall over northeastern India on weekly time scales.

The number of observational studies of effects of aerosols on the large-scale Indian monsoon is also growing. Based on the interannual variability of the TOMS aerosol index (AI), Lau and Kim (2006) found an increase in absorbing aerosol loading over the Indo-Gangetic Plain (IGP) in the pre-monsoon season is associated with anomalous warming related to an anomalous anticyclone circulation in the upper troposphere over the Tibetan Plateau from May to June. As a result, the monsoon season is advanced and rainfall increases in northern India during May-June, consistent with the EHP. Bollasina et al. (2008) emphasized that the excessive absorbing aerosol loading over the Indo-Gangetic Plain (IGP) during May could lead to a reduction in clouds and precipitation due to the semi-direct effect. The reduction in clouds increased solar radiation at the surface, and amplified the land-sea contrast, which in turn lead increase of monsoon precipitation over India in June-July. Gautam et al (2009 a, b) and Gautam et al (2010) provided observational evidence of a multi-decadal warming trend in the mid- and upper troposphere over northwestern India, that is consistent with atmospheric heating due to accumulation of absorbing aerosols over northwestern IGP and the Himalayas. Based on historical data, Lau and Kim (2010) found a 40-year trend of increased rainfall in May-June over northern India that can be attributed to increased aerosols over the IGP. On intraseasonal time scales, Manoj et al. (2011) found that atmospheric heating by absorbing aerosols over central India during long breaks can create a large meridional temperature gradient at low levels between aerosol-rich central India and the pristine equatorial Indian Ocean. They showed that active spells are produced due to the pronounced moisture convergence and deep convection in central India, suggesting that induced positive dynamical feedback can overcome the stability effect caused by solar dimming and possible indirect effects.

While the aforementioned observational studies generally supporting the key premise of the EHP, aspects of the EHP hypothesis remain controversial (Kuhlman and Quaas 2010; Nigam and Bolassina 2011; Lau and Kim 2011). Observational validation of EHP impact on the monsoon is challenging, because EHP involves not only increased aerosol radiative heating, but also dynamical

feedback processes both of which are likely to be strongly influenced by ENSO. The challenge is compounded by the fact that a) monsoon dynamical feedback processes are inherently chaotic, requiring long-term (multi-decadal) data to enhance signal-to-noise ratio, and b) global scale aerosol information rely heavily on satellite data which have a much shorter record (consisting of data segments from heterogeneous measuring instruments with different orbital characteristics), relative to traditional meteorological observations over the Indian monsoon region. Up to now, there has been no observational study that aims at separating aerosol impact relative to ENSO, and possible modulation of ENSO influence by EHP on monsoon responses. This study represent a best-effort attempt, using available satellite aerosol information, in conjunction with rainfall, winds, water vapor, and SST from reanalysis, to provide observational evidence suggesting significant modulation by EHP, on ENSO influence on the Indian monsoon..

2. Data and methods

To maximize the length of the data record, we use four different aerosol datasets to establish the reference time series of aerosol loading for the 33-years base period (1979-2011) chosen for this study. The datasets are 1) NASA Total Ozone Mapping Spectrometer (TOMS) Aerosol Index (AI), 2) Earth Probe (EP) TOMS AI, 3) Moderate Resolution Imaging Spectroradiometer (MODIS)/Aqua, Aerosol Optical Depth (AOD), and 4) MODIS/Terra AOD. TOMS AI and EP TOMS AI with horizontal resolution of 1º by 1.25° are used for the period 1979-1992 and the period 1997-2001, respectively. Positive AI values indicate absorbing aerosols while negative or small AI values indicate non-absorbing aerosols and clouds (Torres et al. 1998; Hsu et al. 1999). MODIS/Terra and MODIS/Aqua with horizontal resolution of 1º by 1º are used for the period 2000-2011 and the period 2003-2011, respectively. MODIS is a key instrument aboard the Terra and Aqua satellites to viewing the entire Earth's surface every 1 to 2 days, acquiring data in 36 spectral bands. Terra's orbit around the Earth is timed so that it passes from north to south across the equator approximately at 10:30 in

the morning, while Aqua passes south to north over the equator approximately 1:30 in the afternoon with a sun-synchronous, near-polar, circular orbit (http://modis.gsfc.nasa.gov/about/). For the overlapping period of Aqua and Terra from 2003 to 2011, the arithmetic average of two AOD values *i.e.*, the mean AOD from each satellite, are used to reduce the bias caused by the different satellite crossing times. For the period 1979-1992, TOMS AI and for the period 1997-2002, EP TOMS was used respectively. A data gap exists during 1993-1996 due to transition of satellite missions from TOMS to EP TOMS. To homogenize the data record for the study period, each dataset is normalized with its standard deviation (Peterson et al. 1998). The normalized data are used to determine years with relatively high and low aerosol loadings within for composite analysis. This process partially alleviates the limitations of the discontinuous data. Note that linear trend in each datasets is not removed because total period of each datasets is too short to consider the linear trend and thereby prevent distorting variability from raw data by artificial removing of linear tend for short period. In the following, the standardized aerosol loading data are referred to as the normalized aerosol index (NAI). GPCP (Global Precipitation Climatology Project) precipitation data (Adler et al. 2003; Huffman et al. 2009) and Nino 3.4 SST data (Smith et al. 2008) are used for the same period as the aerosol data. Temperature, water vapor and winds are from MERRA (Modern Era Retrospective-Analysis for Research and Applications) reanalysis data (Rinecker et al. 2011).

3. Aerosol, rainfall and ENSO relationships

In this Section, we discuss the background information regarding aerosol, rainfall and ENSO relationships to provide the rationale for the approach and methodology used in this study. Figure 1 shows the climatological AI distribution over the greater South Asian monsoon region during the pre-monsoon period from April-May. High aerosol concentrations (high AOD) are found over the Middle East/West Asia, and the Indo-Gangetic Plain (IGP) of northern India. The aerosol concentration decreases rapidly toward southern portions of the Arabian Sea, the Indian subcontinent, the Bay of Bengal and the Indian Ocean. Over Middle East/West Asia, the aerosols comprise mostly of desert

198 dusts. The interannual variation of aerosol over Northern India is highly correlated with high AOD over
199 desert regions of northwestern India and the Arabia Sea, where the dominant aerosol species are dust
200 and sea salt. This is consistent with recent studies (Vinoy et al., 2014, Lau 2014) that on interannual
201 time scales, AOD variation over the northern India is mostly due to transport of dust and sea salt from
202 the Middle East deserts across the Arabian Sea to northern Indian . Over the IGP, the aerosols consist
203 of mostly black carbon (BC) from biomass burning, and from industrial emissions, as well as desert
204 dust transported by monsoon winds from the Middle East and West Asia (Vinoj et al. 2014; Lau 2014).
205 The transport of these aerosols is blocked by the Himalaya foothills. As a result, high aerosol
206 concentration is build up to great heights over the IGP (Gautam *et al*. 2010). Both BC and dust are
207 light absorbing aerosols that can cause heating of the atmosphere. Moreover desert dust over northern
208 India, especially when coated with BC during transport over northern India, can be very absorbing
209 (Ramanathan et al, 2008; Romana et al. 2004). The large north-south gradient of absorbing AOD
210 distribution will induce strong differential heating, and tropospheric temperature gradient between
211 northern Indian and region to the south. The increase in this temperature gradient is essential for
212 triggering the EHP feedback (Lau et al., 2008). The interannual variability of aerosol loading, which is
213 strongly influenced by changing winds and precipitation, is known to be largest over the IGP (Bollasina
214 et al. 2008; Gautam et al. 2009a; Singh et al. 2004; Sanap and Pandithurai 2014). The NAI averaged
215 for April-May and over a large region [70-90 ^{o}E, 20-35 ^{o}N] over northern India (shown as rectangular
216 box in Fig. 1), is used as the reference time series (Fig. 2a) for composite analysis. High and low aerosol
217 years are distinguished according to ± 1σ from the NAI time series. Five high NAI years (i.e., 1988,
218 1991, 2000, 2004, and 2008) and five low NAI years (i.e., 1982, 1983, 1996, 2005, and 2007) were
219 selected for composite analysis with regard to EHP effect on the Indian monsoon. Hereafter, these
220 years are referred to as EHP years. Fig. 2b shows the spatial distribution of the difference in Terra
221 AOD between high years and low years during April to May, indicating clearly that high aerosol
222 concentrations (high AOD) are found over the broaden regions from the northern portions of the
223 Arabian Sea to the Indo-Gangetic Plain (IGP) of northern India. The much higher AOD over the

northern Arabian Sea and desert regions of northwestern India, compared to the densely populated region of the central, and eastern Indo-Gangetic Plain, is an indication that the primary source of aerosols is likely desert dusts transported from the deserts of Middle East, West Asia and northwest India, as found in previous studies (Vinoj et al. 2014; Lau 2014). Note that some EHP years are also ENSO years. A discussion of a methodology to separate EHP and ENSO effects follows.

It is common knowledge that aerosol loading and precipitation are inversely related locally. Aerosols build up under dry, stable and low-wind conditions but are washed out by wet deposition in heavy rain events. It is also well known that Indian monsoon rainfall is affected by ENSO (Rasmussen and Carpenter, 1983, and many others). However most previous studies of monsoon-ENSO relationship are focused on monsoon rainfall during June-July-August. For aerosol impact on monsoon, the building up of aerosols during pre-monsoon period (April-May) before the onset of heavy monsoon rain is critical (Lau et al. 2006). Figure 3 shows the correlation pattern between the negative NINO 3.4 index and precipitation in April-May over the greater South Asian monsoon region. From the signs of the correlations, reduced rainfall is found over a large area that spans the Arabian Peninsula, West Asia and the northwest region of the Indian subcontinent during April-May in La Nina. Increased rainfall is found over large regions of the Indochina Peninsula, the southern South China Sea and the Bay of Bengal, as well as over southwestern Indian subcontinent and the southern Arabian Sea. From an aerosol forcing point of view, it is important to note that during La Nina, large parts of northwestern India, West Asia and Saudi Arabia are drier, *i.e.,* less wet deposition and therefor more favorable for higher aerosol loading. This relationship is consistent with results reported for winter season (Dimri 2012). Note that this is only a necessary but not sufficient condition for increased aerosol loading. Other factors, such as proximity to aerosol sources, wind strength and direction, atmospheric stability, humidity, and topographic effects need to be taken into account for increased aerosol loading.

The relationship between ENSO and aerosol loading over northern India in April-May can be seen in the scatter plot of Nino 3.4 index and NAI (Fig. 4). Here, El Nino years are identified with Nino

3.4 SST> 0.4^{o}C, and La Nina years with SST < -0.4^{o}C. The negative correlation between the Nino 3.4 index and aerosol loading is quite obvious. Three out of four years with highest NAI (>1.0) are La Nina years, and four out of five years with lowest NAI (< -1.0) are El Nino years. All 7 La Nina years exhibiting positive (above normal) NAI, and 6 out of the 9 El Nino years show negative (below) NAI. To investigate the relative impacts of EHP vs. ENSO we select a subset of "pure" ENSO years in which the Nino 3.4 index exceeds ±0.4^{o}C, but with near normal aerosol concentration, *i.e.*, NAI less than ±1.0. As a result, the "pure" El Nino years are: 1987, 1992, 1993, and 1998- and "pure" La Nina years are: 1984, 1985, 1989, and 1999. These subsets of La Nina and El Nino years with near-normal aerosol loading will be referred to as "pure" ENSO (PENSO), where EHP effect is minimized. Notice that there is no overlap between PENSO and EHP years, as indicated above.

4. PENSO vs. EHP effects

Anomalies fields of winds and rainfall (Fig. 5) are constructed based on the differences in the mean of the high and the low NAI (high-minus-low) for EHP, and for PENSO (La Nina minus El Nino) years, respectively. In the following discussion, the sign of the anomalies for PENSO refers to the pure La Nina conditions, and for EHP to high aerosol loading over northern India. During May-June, PENSO anomalous low-level westerly winds are found over extended zonal regions near 5-15^{o}N, stretching from 50^{o}E -120^{o}E (Fig. 5a). The extended zonal anomaly flow appears to be connected to a large-scale anomalous anticyclone, with a broad region of cross-equatorial flow over the Indian Ocean. Pronounced increased rainfall are found over the same zonal belt across the southeastern Bay of Bengal, the Malaysian Peninsular, and regions further east over the South China Sea. Moderate increased rainfall is found, in conjunction with the development of a weak low-level anomalous cyclonic circulation over northeastern India and the northern Bay of Bengal. Rainfall is also slightly increased over the southern Arabian Sea, off the southwestern coast of India. For EHP (Fig. 5c), the May-June wind and rainfall anomalies are similar to PENSO, but the centers of action appear to have shifted from Southeast Asia to northeastern India, and the Bay of Bengal. Here, the westerly anomalies are weaker,

but broader, expanding from 15^{o} N to the equator, compared to PENSO. Strong cross equatorial flow anomalies are confined to the Somali jet off the coast of East Africa. However, low level winds form a well-organized large-scale cyclonic circulation anomaly, around the Arabian Sea, southern India, and the Bay of Bengal, ending with northeasterlies over northern India and the Himalaya foothills. The EHP impact on rainfall over the India subcontinent appears to be more widespread than PENSO, with enhanced rainfall over the Bay of Bengal, northeastern India extending along the Himalayan foothills to northwestern India, and southern Arabian Sea off the coast of southwestern India. The wind and rainfall anomalies for EHP signify a strengthening of the Indian monsoon in the May-June as found in previous studies (Lau and Kim 2006; Lau and Kim 2008).

The subsequent development of the monsoon in July-August is substantially different between PENSO and EHP events. During PENSO July-August (Fig. 5b), the anomalous monsoon flow becomes less organized, featuring anomalous anticyclonic circulation center near southeastern Arabian Sea, and increased westerlies across southern India and the southern Bay of Bengal. Relative to May-June, the zone of increased rainfall has shifted northward to the 20-25^{o} N zonal belt, and anchored to land regions of northern India, Indo-China, and southern China. While rainfall is reduced over the Arabian Sea, and the Bay of Bengal and the Indian Ocean, most regions over northern Indian experience a moderate increase in rainfall. The shifts in anomalous low-level winds and rainfall appear to follow the seasonal northward movement of the monsoon rain belt from early to the mature phase of the monsoon. Overall, for the full seasonal (May-August) mean (not shown), the wind and rainfall patterns indicate a strengthening (weakening) of the Indian monsoon for the La Nina (El Nino) phase of PENSO, in agreement with previous studies (Rasmussen and Carpenter 1983; Kirtman and Shukla 2000; Wang et al. 2001; Wu et al. 2012). Our results show additionally that most of the increased rainfall during La Nina is found in the early monsoon season, May-June. On the other hand, for EHP, weak easterly wind anomalies are found over the Bay of Bengal, central and southern Indian subcontinent (Fig. 5d). Widespread regions of suppressed rainfall are found over India, especially the west and southwest coastal regions. Substantial rainfall suppression is also found over the western

coastal region of Indo-China, and the Malaysian Peninsula. These suggest a weakening of the monsoon in July-August. These patterns are consistent with previous modeling results (Meehl et al. 2008; Collier and Zhang 2009) and observations of long-term trends of Indian rainfall (Gautam et al. 2009b; Lau and Kim 2010), suggesting influence of EHP and related SDM from increased cloudiness induced via EHP atmospheric feedback mechanisms.

To examine the effects of PENSO vs. EHP on the meridional circulation during the pre-monsoon period (May-June), the zonal average latitude-height cross-sections of the wind, temperature, and the specific humidity anomalies over the Indian subcontinent (75-90°E) are shown in Fig. 6. During PENSO, anomalous southerly (northward blowing) winds developed in the lower troposphere blowing from the Indian Ocean to India as a part of a strong large-scale meridional circulation with strong ascending motion, and warming of the troposphere (maxiumum ~1.5-2^{o} C) over northern India and the Himalaya foothills. The meridional overturning is coupled to sinking motion over the equatorial Indian Ocean, and to extensive tropospheric cooling over the Indian Ocean and lower troposphere over central India. Over central India (20-25N), a vertical temperature dipole with warming above and cooling below can be discerned. For EHP, the anomalous meridional circulation is similar to PENSO, but with stronger regional modulations. Compared to PENSO, the meridional cell appears to shift further northward against the Himalaya foothills. The EHP anomalous southerlies form a very thick layer of northerly flow in the lower troposphere and penetrate further inland into northern India, culminating in strong ascending motion over the Himalayan foothills. The warming in the upper troposphere is amplified (maximum~2-2.5^{o}C) and becomes more widespread over northern India and the Tibetan Plateau. Over central India (20-25N), the vertical temperature dipole anomaly is also enhanced. Compared to PENSO, cooling over the Indian Ocean is much reduced. These features are in agreement with EHP induced atmospheric warming (e.g., Lau et al. 2006; Meehl et al. 2008). The strong warming in the middle to upper layers of the troposphere near the Himalaya foothills (~30N), as postulated by EHP is associated with rising warm moist air and increased condensation heating due to increased advection of warm moist air from the Indian Ocean and Arabian Sea. Indeed, Figs. 6c and

6d show that relative to PENSO, EHP induces a larger and deeper moist layer in the lower troposphere to middle troposphere over central and northern India (20-30N).

For PENSO (Fig. 6b), increased easterly zonal wind shear is found in the region 5 ^{o}N-20 ^{o}N, with stronger near surface westerlies, indicating a strengthened large-scale monsoon during La Nina (Webster and Yang 1992). The moistening of the troposphere in northern India appears to be coupled to strong drying over the northern Indian Ocean (0-10 ^{o}N). For EHP, as evident from the large-scale wind shear, the large-scale monsoon is also enhanced for high aerosol over northern India, although the enhancement is not as strong from the large-scale circulation perspective compared to PENSO. This is also seen in the weaker near-surface westerly anomalies in EHP. However, it should be noted that the large-scale monsoon wind shear is affected not only by rainfall (latent heating) over Indian but also by rainfall outside of the India subcontinent, such as over Southeast Asia as in the case of PENSO (Webster and Yang 1992; Krishnamurti et al. 1981). For rainfall over the Indian subcontinent, the EHP effect seems to have a stronger local impact than PENSO. Another major difference between PENSO and EHP is that low-level easterlies are more well-developed over the northern India, near the foothills regions. These low level easterlies could play an important role in bringing moisture from the Bay of Bengal to and initiating heavy rain events over the Himalayan foothills and northwest India (Lau and Kim 2012).

5. Combined impacts ENSO and EHP

As shown in the scatter diagram in Fig. 4, El Nino years with low NAI values and La Nina years with high NAI values are well-separated. In this section, we select the La Nina years with high NAI values (1988, 2000, 2008) and El Nino years with low NAI values (1982, 1983, 1997, 2005) to examine the combined effects (COM), and possible mutual amplification of ENSO and EHP. The COM anomalies is obtained as the difference between composites for these two sets of years. For simplicity, only the May-June composites are shown. The anomalous precipitation and wind patterns induced by the combined effect exhibit features that bear strong similarity to EHP (Fig 7a) except that the zone of

significant increased rainfall is much larger and the magnitude is much enhanced compared to EHP and PENSO alone. Similar to EHP, strongly developed zonal westerly anomaliesare found over 5-15^{o} N extending from 50^{o} E-120^{o} E. Under COM, the atmospheric warming over the Himalayas and the Tibetan Plateau are strongly enhanced (>2.5^{o} C over extensive region in the upper troposphere) and extend to the surface of the Tibetan Plateau (Fig. 7b). The warm-above-cool- below tropospheric temperature dipole over central and northern India becomes very well developed. These results imply that the EHP can mutually modulate and amplify the ENSO effects on summer monsoon rainfall the India subcontinent.

The regional rainfall anomalies in EHP, PENSO and COM are likely associated with changes in convective potential (Wang et al. 2009b; Wang 2013), as reflected in the anomalies of the low-level moist static energy (MSE). The MSE anomalies computed at 850hPa for each of the three cases are shown in Fig. 8 (contour line). Clearly, under PENSO, remote large-scale forcing from La Nina is associated an increase in MSE over northern Indian and the Himalaya foothills. However, the most pronounced signal is the reduced MSE over extensive regions of the Indian Ocean, the Arabian Sea, and the southern Bay of Bengal, as well as the Arabian Peninsular. The inverse relationship between convective potential, and hence rainfall variations over northern India land region, and the oceanic regions to the south are consistent with previous work on intrinsic modes of interannual rainfall variations of the Indian monsoon (Lau et al. 2000). For EHP, the region of positive MSE (increased convective potential) is more expansive compare to PENSO, spanning not only northern India and the Himalaya foothills, but also the entire subcontinent, including the adjacent oceans of the Arabian Sea and the Bay of Bengal. Under COM, the convective potential over the Indian subcontinent is even more enhanced and expansive, as evident in the large positive MSE over northern India and the IGP, and much of the Arabian Sea and the Bay of Bengal. A decomposition of the different terms in the expression for MSE = $C_pT + Lq + gz$, for PENSO, EHP and COM (Fig. 8) shows that the largest contribution to change in MSE is from the moisture term (Lq), much smaller contribution from temperature (C_pT) and negligible amount from potential energy change (gz). Note that the first two

terms of MSE tend to oppose each other, especially in EHP and COM. However, the positive contribution from the moisture term overcomes the negative contribution from the temperature term (C_pT), especially over northeastern India. This suggests that that increase in low level convective instability due to enhanced moisture transport from the Indian Ocean prevails to overcome the stabilization effect due to solar dimming from aerosol and clouds. It is also possible that that the warm/dry and stable condition over the Middle East/West Asia during La Nina in May-June may increase the residence time of dust aerosols in the atmosphere, leading to sustained heating of the atmosphere and strengthening of the prevailing monsoon low-level southwesterly flow (Vinoj et al. 2014; Lau 2014). The enhanced low level flow allows more moisture transport into northern India, and amplifies the ENSO influence through the EHP effect.

The possible amplification and regional modulation of ENSO impacts on Indian monsoon rainfall by EHP can be further quantified by examining the changes in rainfall over northern India (70-95^o E, 20-25^{o}N) and the Himalayan foothill region (15-95^{o}E, 25-30^{o}N) for the early (May-June) and the peak (July-August) monsoon. As shown in Fig. 9, for PENSO May-June, rainfall over both regions are increased by approximately 20-21%, due to the large-scale remote forcing associated with La Nina, but with minimal aerosol impact. For EHP with minimal ENSO impact, rainfall is also increased at a slightly higher percentage of 22-25%. For COM, increase in rainfall at 25-35% is significantly more pronounced compared to PENSO. In all cases, the May-June rainfall increase in northern India is stronger than in the foothills region. The changes are highly significant exceeding 1% confidence level, especially for EHP and COM, based on Student's t-test. Interestingly, in July-August, PENSO does not have a significant impact on rainfall over the two regions (Fig. 9b), whereas EHP increases (decreases) rainfall in the foothills (northern India) at about 5%. In COM, when EHP combined with ENSO effects, rainfall over the foothill regions is further enhanced (~14%), marginally significant at 10% confidence level, while over northern India, the reduction remained at approximately 5%. It should be pointed out that because of the intensity and total rain amount is much higher during the peak monsoon, the same percentage change in rainfall would mean a much larger absolute amount of rainfall.

406 A 14% increase in rainfall during the active monsoon spell in the foothill regions could spell major
407 disaster.
408
409 **6. Summary Discussions**
410 In this study, we present observational evidence of amplification of ENSO influence on the Indian
411 summer monsoon by, and regional forcing from absorbing aerosols via EHP and related feedback
412 processes. Results are obtained based on high-minus-low composite analysis carried out separately
413 for a) PENSO, *i.e.*, ENSO years with normal NAI over northern India, b) EHP, *i.e.*, years with NAI
414 exceeding one standard-deviation, and c) COM, *i.e.*, combined effects of La Nina (El Nino) years and
415 high (low) AOD years. Key findings include:
416 - On interannual time scales, La Nina (El Nino) is associated with high (low) AOD over
417 northwestern India and the northern Arabia Sea, during the pre-monsoon period (April-May),
418 indicative of desert dusts as the primary source of aerosols.
419 - During PENSO La Nina years, the Indian monsoon is strengthened with increased rainfall over
420 northeastern India in May-June, in association with an enhanced meridional circulation with
421 anomalous rising motion, over northern India and anomalous sinking motion over southern
422 India and the North Indian Ocean.
423 - During EHP years, the basic response is similar to PENSO, except that the magnitude of the
424 anomalous rainfall and rising motion is stronger over the Himalaya foothills and the Bay of
425 Bengal in May-June. The increased rainfall appears to be associated with, increased moisture
426 transport from the Arabian Sea and Indian Ocean to northern Indian and the Bay of Bengal by
427 way of well-organized large-scale low-level cyclonic circulation encompassing the entire
428 Indian subcontinent and adjacent oceans. This is followed by a weakened monsoon with
429 suppressed rainfall, and reduced low level westerlies over the Indian subcontinent in July-
430 August, consistent with a scenarios postulated by EHP and related effects (Lau et al. 2010;
431 Meehl et al. 2008).

- Under the combined effects of ENSO and strong EHP forcing in COM, the increased rainfall in May-June over northern India and the Himalayas foothills are substantially amplified compared to PENSO and EHP. Specifically, May-June rainfall over the Indo-Gangetic Plain is increased by 25-30%, compared to ~20 % for PENSO. In July-August, rainfall over the Himalayan foothills increases by 14%, but slightly reduced over the eastern IGP, compared to no significant signals during PENSO.

The key findings suggest that the EHP effect by absorbing aerosol may play an important role in amplifying the ENSO influence on the Indian monsoon. The present results are also consistent with previous findings (Vinoj et al. 2014; Lau 2014) that on fast time scales (1-2 weeks) the build up of aerosols over northern Indian and the Arabian Sea in the pre-monsoon season is likely to be from long-range transport of dusts from deserts of the Middle East, and West Asia regions. These dust aerosols are strong absorbers of solar radiation, especially when coated with fine black carbon aerosols as they pass over densely populated and highly industrial complex of the Indo-Gangetic Plain (Srivastava and Ramachandran 2012; Kedia et al. 2014). As a result, strong heating of the atmosphere by the mixture of dust and black carbon can induce or trigger EHP-like diabatic heating feedback, altering the subsequent evolution of the Indian monsoon (Lau et al. 2009). Additionally, the emission of dust aerosols from the desert surface, and their transport to northern India are strongly dependent on strength of the southwest monsoon winds, which are also strongly influenced by ENSO (Lau et al. 2008) Since the EHP effects are highly nonlinear, requiring aerosol concentration over the IGP and the foothills regions to build-up to a critical loading, such that the anomalous heating from EHP can overcome the stability effect due to the aerosol semi-direct effect, it is possible that the ENSO may serve as an important forcing agent that operates as a triggering mechanism trigger for the EHP effect during the pre- and early monsoon season. Once, the trigger is activated, the EHP and related feedback processes including aerosol microphysics effects may further modulate the Indian monsoon response to ENSO forcing. The EHP effect, being intrinsically fast (days to weeks) atmospheric processes, will be in quasi-equilibrium with, and contribute to the changing coupled atmosphere-land-ocean system in the

458 monsoon regions, manifesting in regional ENSO-aerosol feedbacks on seasonal, interannual and
459 possibly climate change time scales.

460 For individual years, the main features identified from the composite can be seen, but not as clearly as
461 in the composite. It is because of possible influence factors on interannual variability of the monsoon
462 rainfall. These include case-by-case differences in ENSO strengths and evolutions, and associated
463 dust and moisture transport, phase and amplitude of the Indian Ocean Dipole (IOD), local sea surface
464 temperature anomalies and feedbacks, snow cover over Eurasia, as well as natural
465 variability(Achuthavarier et al. 2012; Cherchi and Navarra 2013). Thus it should be noted that the
466 impact of specific factor for each individual year cannot be isolated easily due to uneven interference
467 of other factors.

468 On the other hand, there are several works about an obvious weakening of ISM-ENSO relationship in
469 the late 1970s which is related to mean state change (Krishna Kumar et al. 1999), impact of Indian
470 Ocean Dipole (Ashok et al. 2004), change in the SST anomaly pattern in equatorial Pacific (Krishna
471 Kumar et al. 2006; Ashok et al. 2007), and many others. Recently, Wu et al. (2012) showed that ENSO-
472 ISM relationships depend on three types of ENSO influences on the Indian Summer Monsoon(ISM)
473 and there is the observed weakening in the ISM-ENSO relationship around the late 1970s in the type of
474 DJF & JJAS cases which is corresponding to coherent influence of both the preceding winter and
475 concurrent summer eastern equatorial Pacific SST anomalies. It is not clear whether the observed
476 weakening is linked to EHP effect because this study focused on ENSO-EHP links. This topic should
477 be explored as a challenging topic along with global warming and associated dryness/wetness including
478 IOD-EHP links in the future study.

479 **Acknowledgements**

480 This work was funded by the Korea Meteorological Administration Research and Development
481 Programunder grant KMIPA2015-2085. Partial support was provided by the GSFC Strategic Science
482 Support, and the NASA Interdisciplinary (IDS) Investigations.
483

Conflict of interest: None

485 **References**

486 Achuthavarier D, Krishnamurthy V, Kirtman BP, Huang B (2012) Role of the Indian Ocean in the
487 ENSO–Indian Summer Monsoon Teleconnection in the NCEP Climate Forecast System. J Clim,
488 25: 2490–2508. doi: http://dx.doi.org/10.1175/JCLI-D-11-00111.1

489 Adler RF, Huffman GJ, Chang A, Ferraro R, Xie P, Janowiak J, Rudolf B, Schneider U, Curtis S, Bolvin
490 D, Gruber A, Susskind J, Arkin P (2003) The Version 2 Global Precipitation Climatology Project
491 (GPCP) Monthly Precipitation Analysis (1979-Present). J Hydrometeor 4:1147-1167Ashok K,
492 Guan Z, Saji NH, Yamagata T (2004) On the individual and combined influences of the ENSO
493 and the Indian Ocean dipole on the Indian summer monsoon. J Cim 17: 3141– 3155

494 Ashok K, Behera SK, Rao SA, Weng H, and Yamagata T (2007) El Nin ˜o Modoki and its possible
495 teleconnection. J Geophys Res 112:C11007. doi:10.1029/2006JC003798

496

497 Bellouin N, Boucher O, Haywood J, Reddy MS (2005) Global estimate of aerosol direct radiative
498 forcing from satellite measurements. Nature 438:1138–1141

499 Bollasina M, Nigam S (2011) Absorbing aerosols and pre-summer monsoon hydroclimate variability
500 over the Indian subcontinent: The challenge in investigating links. Atmos Res 94:338–344.
501 doi:10.1016/j.atmosres.2009.06.008

502 Bollasina M, Nigam S, Lau KM (2008) Absorbing aerosols and summer monsoon evolution over South
503 Asia: An observational portrayal. J Clim 21:3221–3239. doi:10.1175/2007JCLI2094.1

504 Bollasina MA, Ming Y, Ramaswamy V (2011) Anthropogenic aerosols and the weakening of the South
505 Asian summer monsoon. Science 334:502–505. doi:10.1126/science.120499

506 Bollasina MA, Ming Y, Ramaswamy V (2013) Earlier onset of the Indian monsoon in the late twentieth
507 century: The role of anthropogenic aerosols. Geophys Res Lett 40:3715–3720
508 doi:10.1002/grl.50719

509 Cherchi A, Navarra A (2013) Influence of ENSO and of the Indian Ocean Dipole on the Indian summer
510 monsoon variability. Clim Dyn 41:81–103. DOI 10.1007/s00382-012-1602-y

511 Chung CE, Ramanathan V, Kiehl JT (2002) Effects of the south-Asian absorbing haze on the northeast
512 monsoon and surface-air heat exchange. J Clim 15:2462–2476
513 Chung CE, Ramanathan V (2006) Weakening of north Indian SST gradients and the monsoon rainfall
514 in India and the Sahel. J Clim 19:2036– 2045. doi:10.1175/JCLI3820.1
515 Collier JC, Zhang GJ (2009) Aerosol direct forcing of the summer Indian monsoon as simulated by the
516 NCAR CAM3. Clim Dyn 32:313–332. doi:10.1007/s00382-008-0464-9
517 Cowan T, Cai W (2011) The impact of Asian and non-Asian anthropogenic aerosols on 20th century
518 Asian summer monsoon. Geophys Res Lett 38:L11703. doi:10.1029/2011GL047268
519 Dimri AP (2012) Relationship between ENSO phases and northwest India winter precipitation. Int J
520 Climatol 33: 1917-1923. doi:10.1002/joc.3559
521 Ganguly D, Rasch PJ, Wang H, Yoon JH (2012) Climate response of the South Asian monsoon system
522 to anthropogenic aerosols. J Geophys Res 117:D13209. doi:10.1029/2012JD017508
523 Gautam R, Hsu NC, Lau KM, Kafatos M (2009a) Aerosol and rainfall variability over the Indian
524 monsoon region: Distributions, trends and coupling. Ann Geophys 29: 3691–3703
525 Gautam R, Hsu NC, Lau KM, Tsay SC, Kafatos M (2009b) Enhanced pre-monsoon warming over the
526 Himalayan-Gangetic region from 1979 to 2007. Geophys Res Lett, 36, L07704,
527 doi:10.1029/2009GL037641
528 Gautam R, Hsu NC, Lau KM (2010) Premonsoon aerosol characterization and radiative effects over the
529 Indo-Gangetic Plains: Implications for regional climate warming. J Geophys Res, 115, D17208,
530 doi:10.1029/2010JD013819
531 Haywood J, Boucher O (2000) Estimates of the direct and indirect radiative forcing due to tropospheric
532 aerosols: a review. Rev Geophys 38:513–543. doi:10.1029/1999RG000078
533 Hsu NC, Herman JR, Torres O, Holben BN, Tanre D, Eck TF, Smirnov A, Chatenet B, and Lavenu F
534 (1999) Comparisons of the TOMS aerosol index with Sun-photometer aerosol optical thickness:
535 Results and applications. J Geophys Res, 104(D6): 6269–6279.

536 Huffman, GJ, Adler RF, Bolvin DT, Gu G (2009) Improving the Global Precipitation Record: GPCP
537 Version 2.1. Geophys Res Lett 36, L17808. doi:10.1029/2009GL040000
538 Jacobson MZ (2001) Strong radiative heating due to the mixing state of black carbon in atmospheric
539 aerosols. Nature 409:695–698
540 Kedia S, Ramachandran S, Holben BN, Tripathi SN (2014) Quantification of aerosol type, and sources
541 of aerosols over the Indo-Gangetic Plain. Atmos Environ 98:607-619.
542 http://dx.doi.org/10.1016/j.atmosenv.2014.09.022
543 Kerr RA, (2007) Pollutant hazes extend their climate-changing reach. Science 315: 1217-1217. DOI:
544 10.1126/science.315.5816.1217
545 Kim D, Wang C, Ekman AML, Barth MC, Rasch P (2008) Distribution and direct radiative forcing of
546 carbonaceous and sulfate aerosols in an interactive size-resolving aerosol-climate model. J
547 Geophy Res 113:D16309. doi:10.1029/2007JD009756
548 Kim MK, Lau WKM, Chin M, Kim KM, Sud YC, Walker GK (2006) Atmospheric teleconnection over
549 Eurasia induced by aerosol radiative forcing during boreal spring. J Clim 19:4700–4718.
550 doi:10.1175/JCLI3871.1
551 Kirtman B, Shukla J (2000) Influence of the Indian summer monsoon on ENSO. Q J R Meteorol Soc
552 126: 213-239
553 Krishna Kumar K, Rajagopolan B, Cane MA (1999) On the weakening relationship between the Indian
554 monsoon and ENSO. Science 284: 2156–2159. DOI: 10.1126/science.284.5423.2156
555 Krishna Kumar K, Rajagopolan B, Hoerling M, Bates G, Cane M (2006) Unraveling the mystery of
556 Indian monsoon failure during El Nino. Science 314:115–119. DOI: 10.1126/science.1131152
557 Krishnamurti TN, Ardanuy P, Ramanathan Y, Pasch R (1981) On the onset vortex of the summer
558 monsoon. Mon Wea Rev 109: 344-363
559 Kuhlmann J, Quaas J (2010) How can aerosols affect the Asian summer monsoon? Assessment during
560 three consecutive pre-monsoon seasons from CALIPSO satellite data. Atmospheric Chemistry
561 and Physics 10: 4673-4688

562 Lau KM, Kim KM, Yang S (2000) Dynamical and Boundary Forcing Characteristics of Regional
563 Components of the Asian Summer Monsoon. J Clim13: 2461–2482
564 Lau KM (2014) Desert dust and monsoon rain. Nat Geosci 7:255–256. doi:10.1038/ngeo2115
565 Lau KM, Kim KM (2006) Observational relationships between aerosol and Asian monsoon rainfall,
566 and circulation. Geophys Res Lett 33:L21810. doi:10.1029/2006GL027546
567 Lau KM, Kim MK, Hsu C, Holben B (2009) Possible influences of air pollution, dust and sandstorms
568 on the Indian monsoon. *WMO Bulletin* **58 (1):** 22-30
569 Lau KM, Kim KM (2010) Fingerprinting the impacts of aerosols on long-term trends of the Indian
570 summer monsoon regional rainfall. Geophys Res Lett 37 (16): L16705.10.1029/2010GL043255
571 Lau KM, Kim KM (2011) Comment on "'Elevated heat pump' hypothesis for the aerosol-monsoon
572 hydroclimate link: 'Grounded' in observations?" by S. Nigam and M. Bollasina. J Geophys
573 Res 116, D07203, doi:10.1029/2010JD014800
574 Lau KM, Kim KM (2012) The 2010 Russian Heat Wave/Wildfires and Pakistan Flood: Teleconnection
575 of Extremes. J Hydrometeor 13, 392-403 doi:10.1175/JHM-D-11-016.1
576 Lau KM, Kim MK, Kim KM (2006) Aerosol induced anomalies in the Asian summer monsoon: the
577 role of the Tibetan Plateau. Clim Dyn 26:855–864. doi:10.1007/s00382-006-0114-z
578 Lau KM, et al (2008) The Joint Aerosol-Monsoon Experiment: a new challenge for monsoon climate
579 research. Bull Amer Meteor Soc 89:369–383. doi:10.1175/BAMS-89-3-369
580 Lau KM, Kim MK, Kim KM, Lee WS (2010) Enhanced surface warming and accelerated snow melt in
581 the Himalayas and Tibetan Plateau induced by absorbing aerosols. Environ Res Lett 5 025204
582 doi: 10.1088/1748-9326/5/2/025204
583 Manoj MG, Devara PCS, Safai PD, Goswami BN (2011) Absorbing aerosols facilitate transition of
584 Indian monsoon breaks to active spells. Clim Dyn 37:2181–2198. doi:10.1007/s00382-010-
585 0971-3

586 Meehl GA, Arblaster JM, Collins WD (2008) Effects of black carbon aerosols on the Indian monsoon.
587 J Clim 21:2869–2882. doi:10.1175/2007JCLI1777.1
588 Menon S, Hansen J, Nazarenko L, Luo Y (2002) Climate effects of black carbon aerosols in China and
589 India. Science 297:2250–2253
590 Nigam S, Bollasina M (2011) Reply to comment by K. M. Lau and K. M. Kim on "'Elevated heat
591 pump' hypothesis for the aerosol–monsoon hydroclimate link: 'Grounded' in observations?". J.
592 Geophys. Res., 116, D07204, doi:10.1029/2010JD015246
593 Peterson TC, Easterling DR, Karl TR, Groisman P, Nicholls N, Plummer N, Torok S, Auer I, Boehm
594 R, Gullett D, Vincent L, Heino R, Tuomenvirta H, Mestre O, Szentimrey T, Salinger J, Forland
595 E, Hanssen-Bauer I, Alexandersson H, Jones P, Parker D (1998) Homogeneity adjustments of
596 *in situ* atmospheric climate data: a review. Int J Climatol **18***:* 1493–1517
597 Ramana MV, Ramanathan V, Podgorny IA, Pradhan BB, Shrestha B (2004) The direct observations of
598 large aerosol radiative forcing in the Himalayan region. Geophys Res Lett 31:L05111.
599 doi:10.1029/2003GL018824
600
601 Ramanathan V, Chung C, Kim D et al (2005) Atmospheric brown clouds: Impact on South Asian
602 climate and hydrologic cycle. Proc Natl Acad Sci U S A 102:5326–5333.
603 doi:10.1073/pnas.0500656102
604 Ramanathan V, Crutzen PJ, Lelieveld J et al (2001) Indian Ocean Experiment: an integrated analysis of
605 the climate forcing and effects of the great Indo-Asian haze. J Geophys Res 106:28371–28398
606 Ramanathan V, Carmichael G (2008) Global and regional climate changes due to black carbon. Nat
607 Geosci 1:221-227, 2008. doi:10.1038/ngeo156
608 Randles CA, Ramaswamy V (2008) Absorbing aerosols over Asia: a Geophysical Fluid Dynamics
609 Laboratory general circulation model sensitivity study of model response to aerosol optical
610 depth and aerosol absorption. J Geophys Res 113:D21203. doi:10.1029/2008JD010140

611 Rasmusson EM, Carpenter TH (1983) The relationship between eastern equatorial Pacific sea surface
612 temperature and summer monsoon rainfall over India and Sri-Lanka. Mon Wea Rev 111: 517-
613 528
614 Rienecker MM, Suarez MJ, Gelaro R et al (2011) MERRA: NASA's modern-era retrospective analysis
615 for research and applications. J Clim 24:3624–3648. doi:10.1175/JCLI-D-11-00015.1
616 Sanap SD, Pandithurai G (2014) Inter-annual variability ofaerosols and its relationship with regional
617 climate over Indian subcontinent. Int J Climatol doi:10.1002/joc.4037
618 Singh RP, Dey D, Tripathi SN, Tare V, Holben B (2004) Variability of aerosol parameters over
619 Kanpur, northern India. J Geophys Res 109, D23206. doi:10.1029/2004JD004966
620 Smith TM, Reynolds RW, Peterson TC, and Lawrimore J (2008) Improvements to NOAA's Historical
621 Merged Land–Ocean Surface Temperature Analysis (1880–2006). J Clim 21: 2283–2296
622 Srivastava R, Ramachandran S (2012) The mixing state of aerosols over the Indo-Gangetic Plain and
623 its impact on radiative forcing. Q J R Meteorol Soc 139:137-151. doi:10.1002/qj.1958
624 Torres O, Bhartia PK, Herman JR, Ahmad Z, Gleason J (1998) Derivation of aerosol properties from
625 satellite measurements of backscattered ultraviolet radiation: Theoretical basis. J Geophys Res
626 103(D14): 17,099– 17,110
627 Vinoj V, Rasch PJ, Wang H, Yoon JH, Ma PL, Landu K (2014) Short-term modulation of Indian summer
628 monsoon rainfall by West Asian dust. Nat Geosci 7:308–313. doi:10.1038/ngeo2107
629 Wang B, Wu R, Lau KM (2001) Interannual variability of the Asian summer monsoon: Contrasts
630 between the Indian and the western North Pacific–East Asian monsoons. J. Climate, 14:4073–
631 4090
632 Wang C (2013) Impact of anthropogenic absorbing aerosols on clouds and precipitation: a review of
633 recent progresses. Atmos Res 122:237–249. doi:10.1016/j.atmosres.2012.11.005
634 Wang C, Jeong GR, Mahowald N (2009a) Particulate absorption of solar radiation: anthropogenic
635 aerosols vs. dust. Atmos Chem Phys 9:3935–3945

636 Wang C, Kim D, Ekman AML, Barth MC, Rasch PJ (2009b) Impact of anthropogenic aerosols on
637 Indian summer monsoon. Geophys Res Lett 36:L21704. doi:10.1029/2009GL040114
638 Webster PJ, Yang S (1992) Monsoon and ENSO: Selectively interactive systems. Q J R Meteorol Soc
639 118: 877-926
640 Wu R, Chen J, Chen W (2012) Different Types of ENSO Influences on the Indian Summer Monsoon
641 Variability. J Clim 25: 903–920. doi: http://dx.doi.org/10.1175/JCLI-D-11-00039.1

642

643

644 **Figure Legends**

645 **Fig. 1** April-May climatological (1988, 1991, and 2000) distribution for the high aerosol index (AI)
646 years and representative area for the selected cases (black box)

647 **Fig. 2 (a)** Time series of the normalized aerosol index (NAI) from the TOMS AI, Aqua AOD, and Terra
648 AOD datasets, and (b) April-May the difference in Terra AOD between high years and low years.

649 **Fig. 3** Correlation pattern between negative Nino 3.4 SST and precipitation during the period April-
650 May

651 **Fig. 4** Scatter diagram between the NAI and the NINO 3.4 SST during April-May.. El Nino, La Nina,
652 and normal years are indicated by blue, red and open circles. Number inside circles denotes the
653 calendar year.

654 **Fig. 5** Changes in precipitation and wind for PENSO (top panel) and EHP (bottom panel) effects for
655 May-June (left panel) and July-August (right panel). Large and small circles represent significance level
656 of 1 and 5%, respectively.

657 Fig. 6 Changes in zonal mean (75-90°E) temperature and streamfunction (left panel) and specific
658 humidity and zonal winds (right panel) for PENSO (top panel) and EHP (bottom panel) for May-June.
659 Large and small circles represent significan**c**e level of 1 and 5%, respectively.

660 **Fig. 7** Changes in (a) precipitation and 850 hPa wind and (b) zonal mean (75-90°E) temperature and
661 streamfunction (right, 75-90°E) for COM (ENSO with abnormal NAI years) for May-June. Large and
662 small circles represent significance level of 1 and 5%, respectively.

663 **Fig. 8** Changes in moist static energy (MSE) (contour) for PENSO (top row), EHP (middle row), and
664 COM (bottom row) for May-June at 850 hPa. Shading in left, middle and right panel represent three
665 terms (C_PT, Lq, and gz) of the MSE, respectively. Unit of MSE is in 10^3 J/kg.

666 **Fig. 9** Changes in precipitation (color bars) induced by the PENSO, EHP, and combined (COM) effects
667 for (a) May-June and (b) July-Aug. Vertical Error line bars represent mean standard error of change in
668 precipitation. Green denotes the Himalayan foothills (25-30°N, 75-95°E); yellow denotes the Indo-
669 Gangetic Plain(20-25°N, 75-95°E)

670

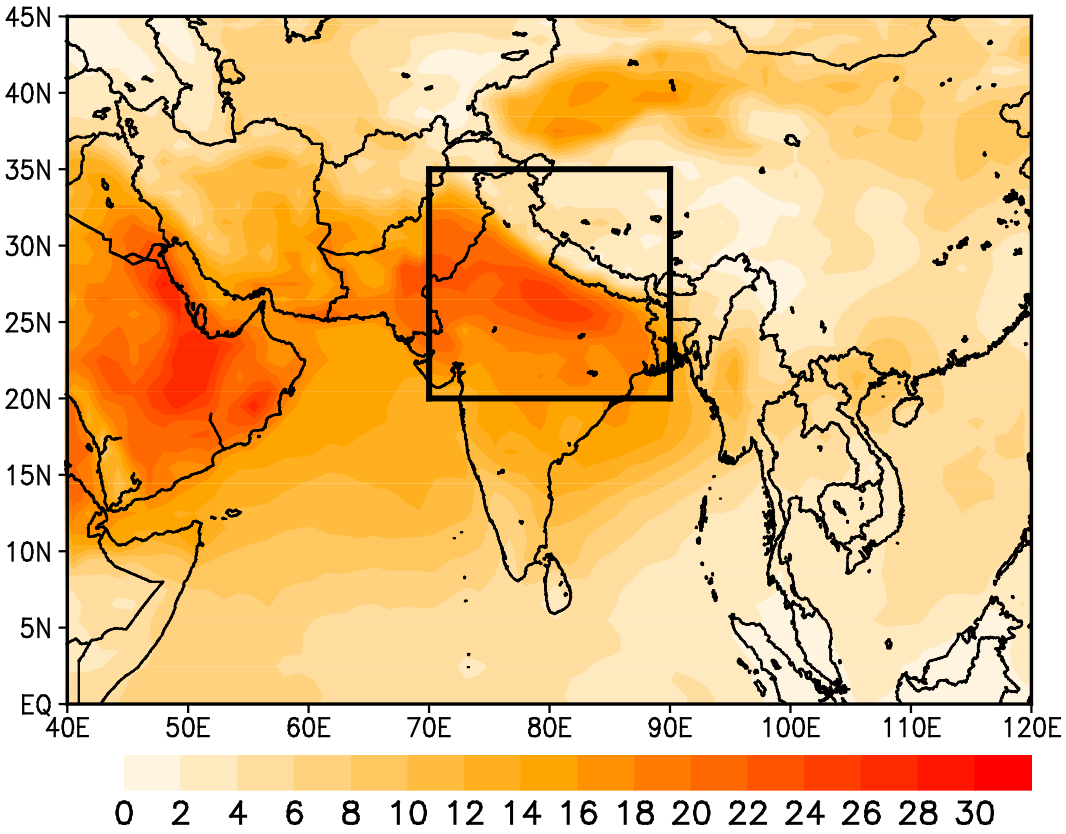

671

672 **Fig. 1** April-May climatological (1988, 1991, and 2000) distribution for the high aerosol index (AI)
673 years and representative area for the selected cases (black box)

674

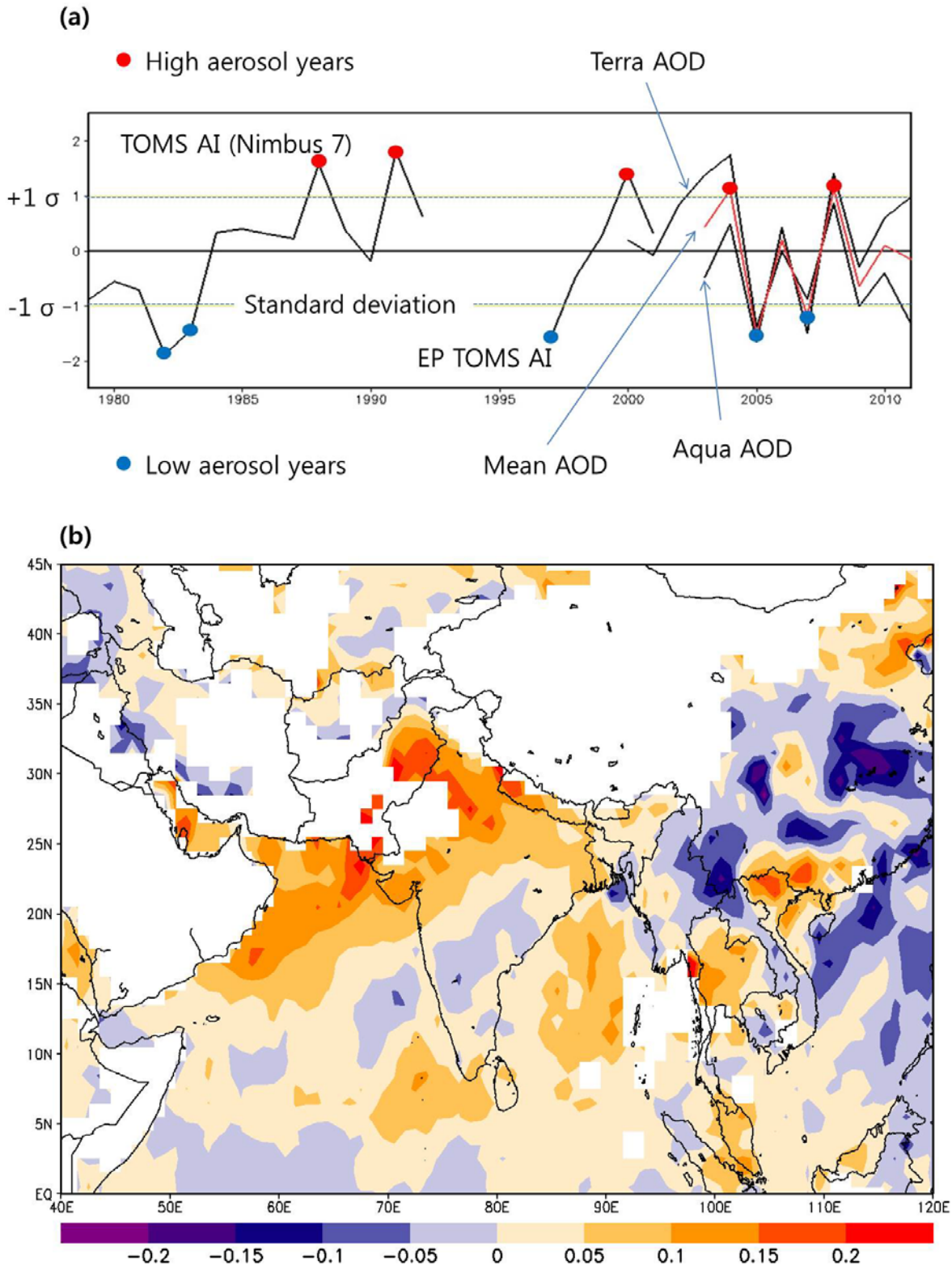

Fig. 2 (a) Time series of the normalized aerosol index (NAI) from the TOMS AI, Aqua AOD, and Terra AOD datasets, and (b) April-May the difference in Terra AOD between high years and low years.

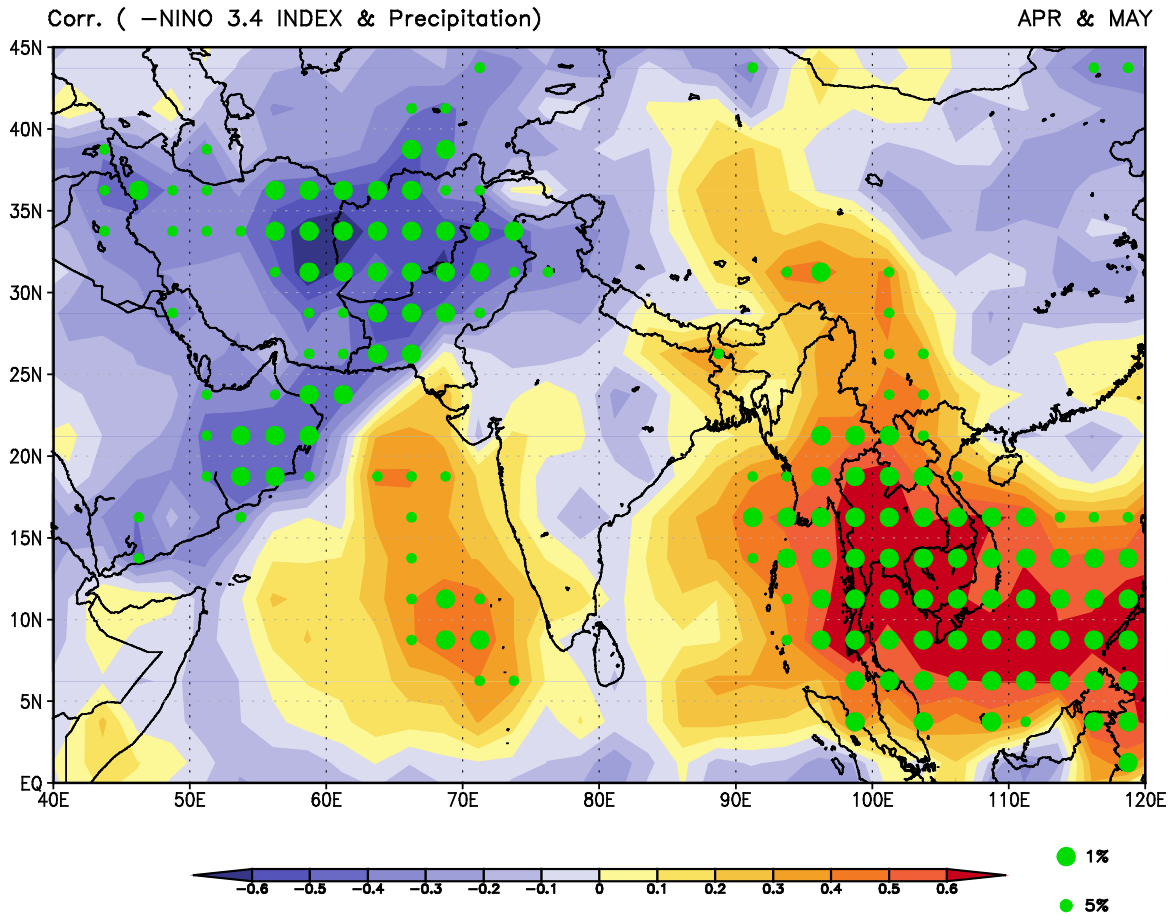

680

681 **Fig. 3** Correlation pattern between negative Nino 3.4 SST and precipitation during the period April-
682 May

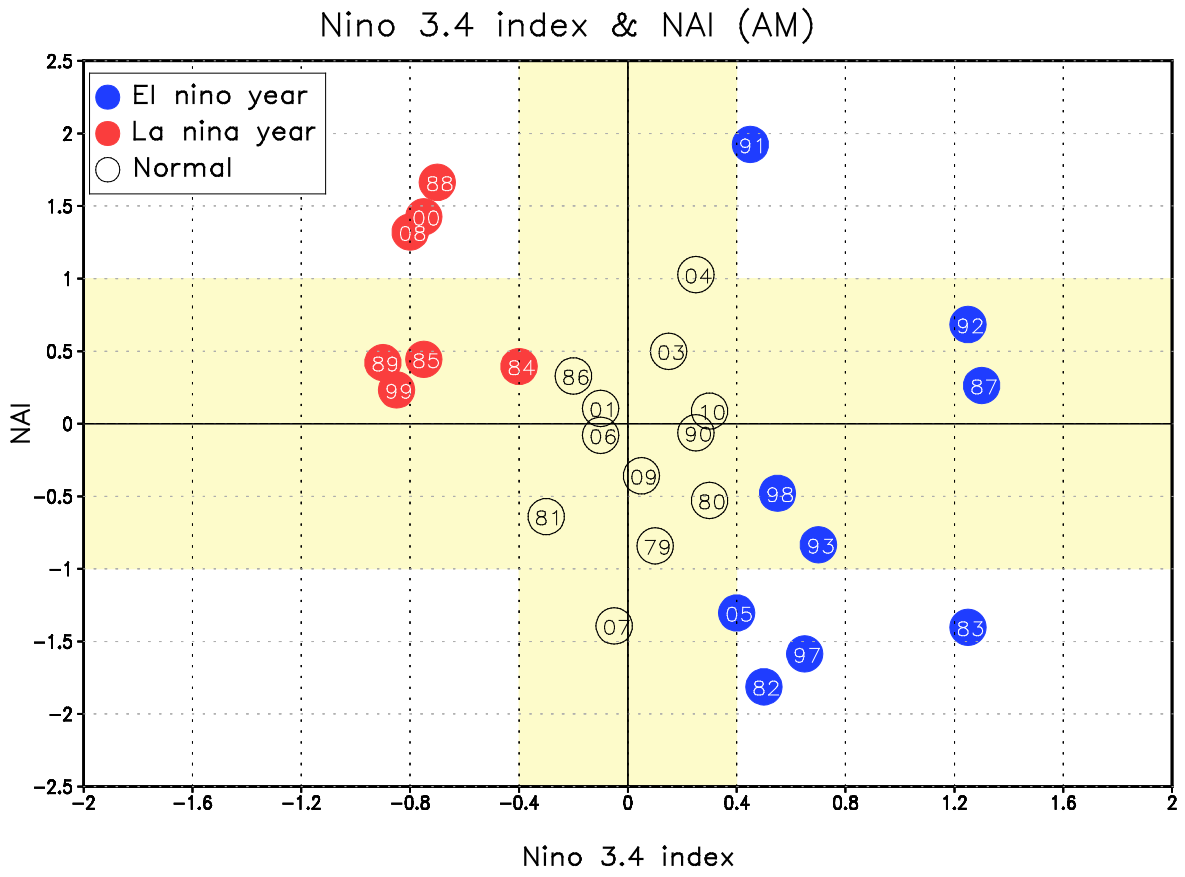

683

684 **Fig. 4** Scatter diagram between the NAI and the NINO 3.4 SST during the period April-May. El Nino,
685 La Nina, and normal years are indicated by blue, red and open circles. Number inside circles denotes
686 the calendar year.

687

688

689

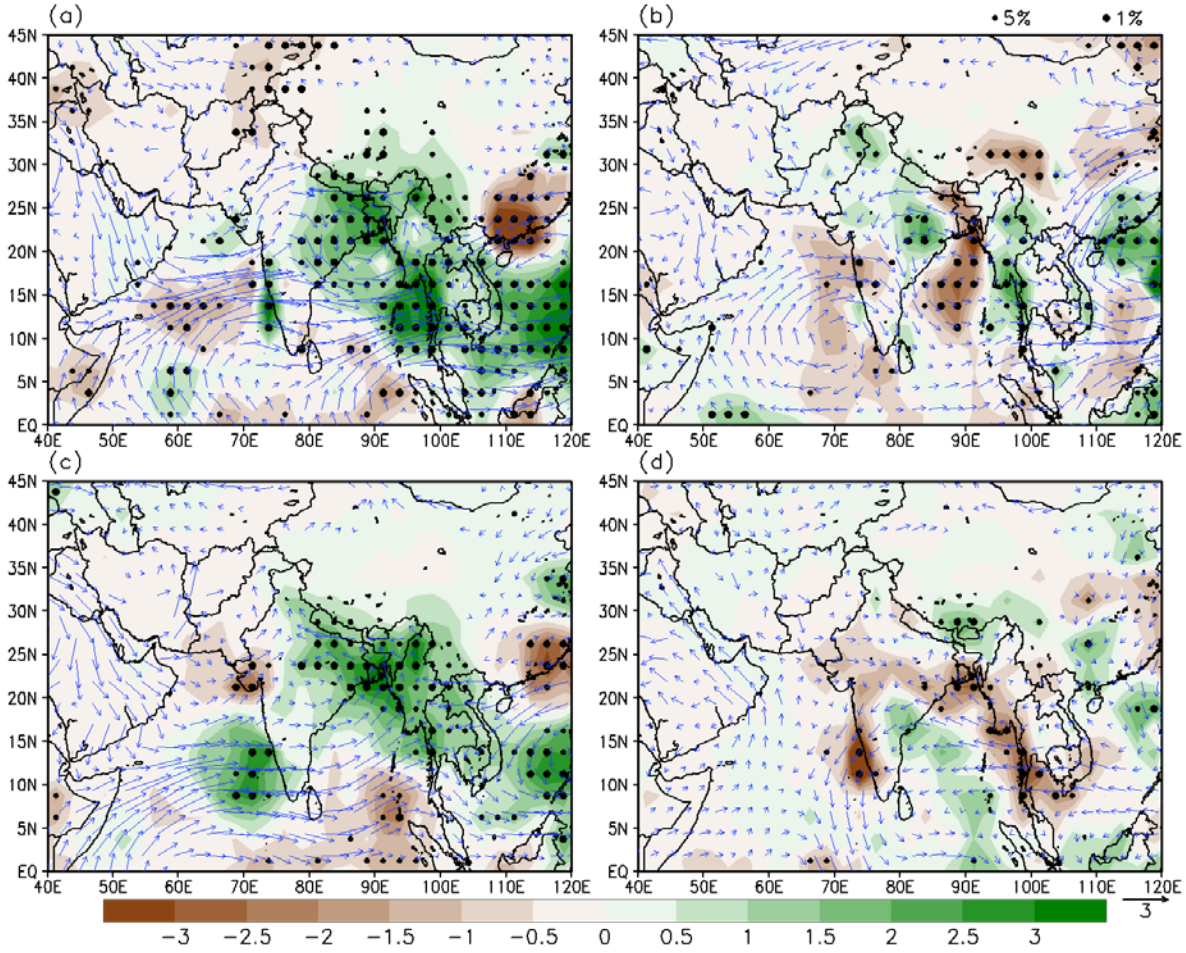

690

691 **Fig. 5** Changes in precipitation and wind for PENSO (top panel) and EHP (bottom panel) effects for
692 May-June (left panel) and July-August (right panel). Large and small circles represent significance level
693 of 1 and 5%, respectively.

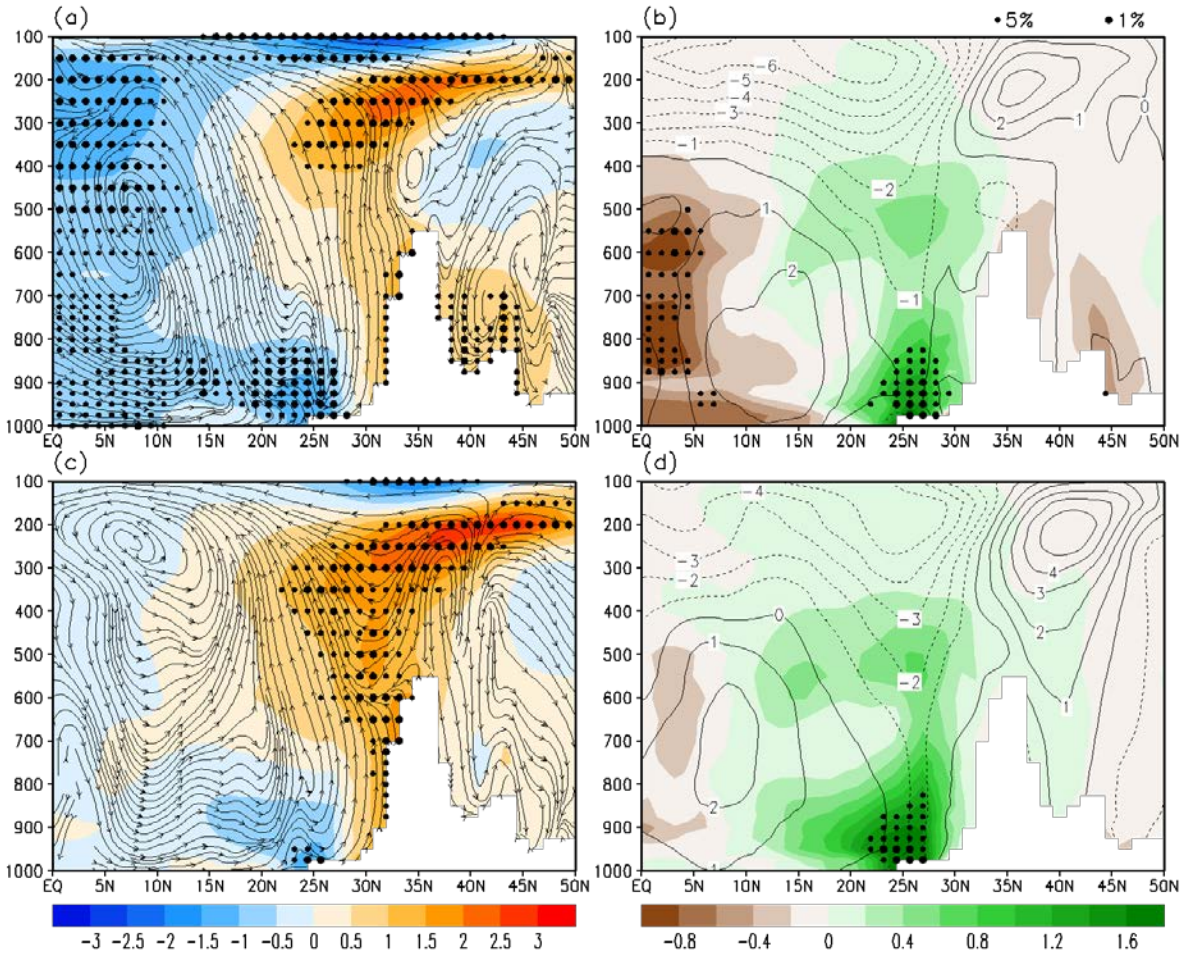

694

695 **Fig. 6** Changes in zonal mean (75-90°E) temperature and stream function (left panel) and specific
696 humidity and zonal wind (right panel) for PENSO (top panel) and EHP (bottom panel) effects for May-
697 June. Large and small circles represent significance level of 1 and 5%, respectively.

698

699

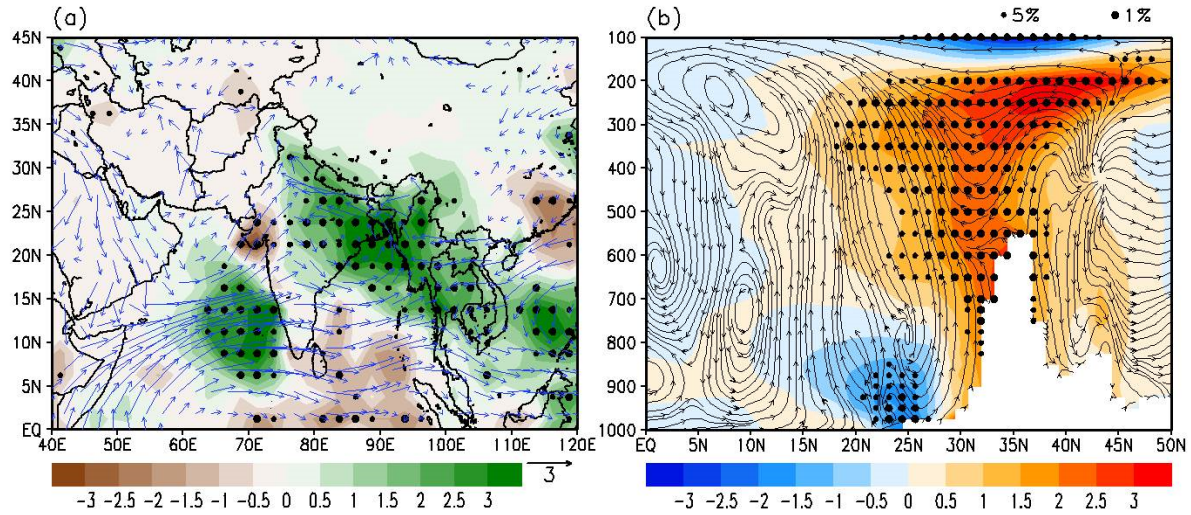

700

701 **Fig. 7** Changes in (a) precipitation and 850 hPa wind and (b) zonal mean (75-90°E)temperature and
702 stream function (right, 75-90°E) for COM (ENSO with abnormal NAI years) for May-June. Large and
703 small circles represent significance level of 1 and 5%, respectively.

704

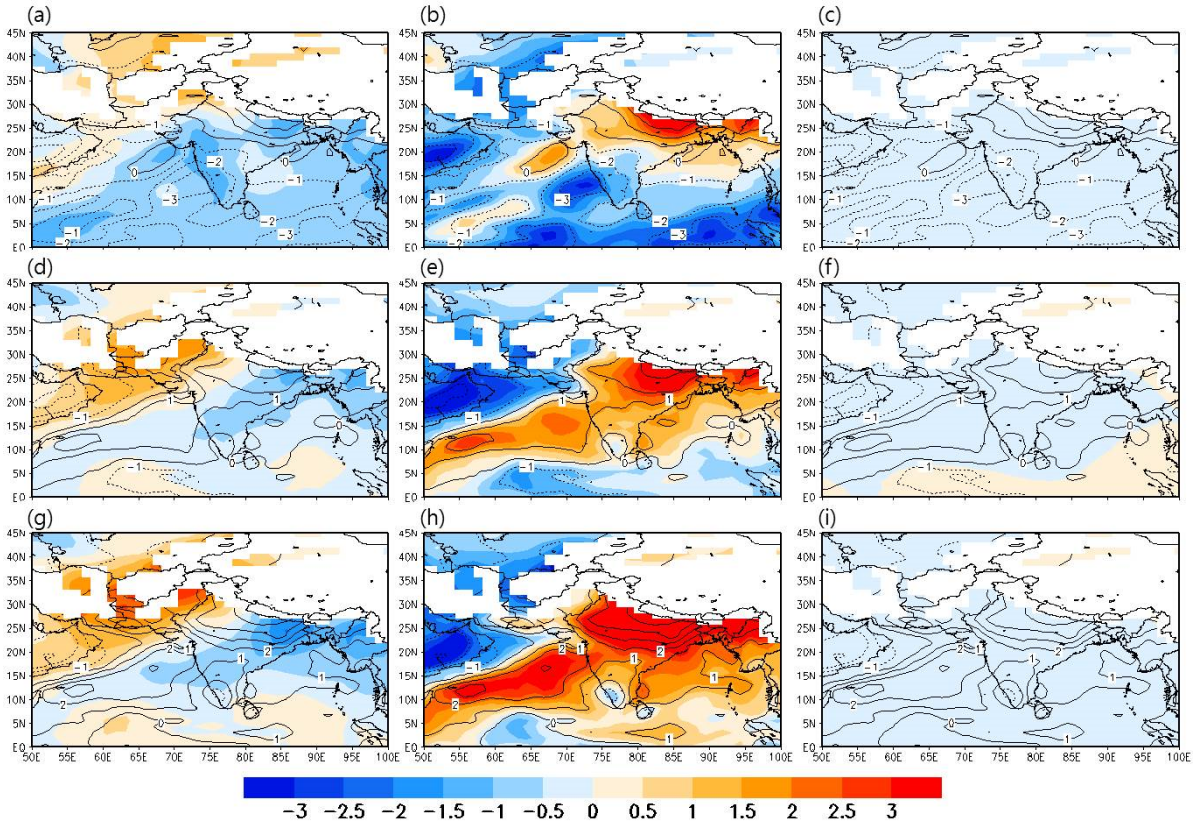

Fig. 8 Changes in moist static energy (MSE) (contour) for (a) PENSO (top low), (b) EHP (middle low), and (c) COM (bottom low) effects for May-June at 850 hPa. Shading in left, middle and right panel represent three terms (C_PT, Lq, and gz) of the MSE, respectively. Unit of MSE is in 10^3 J/kg.

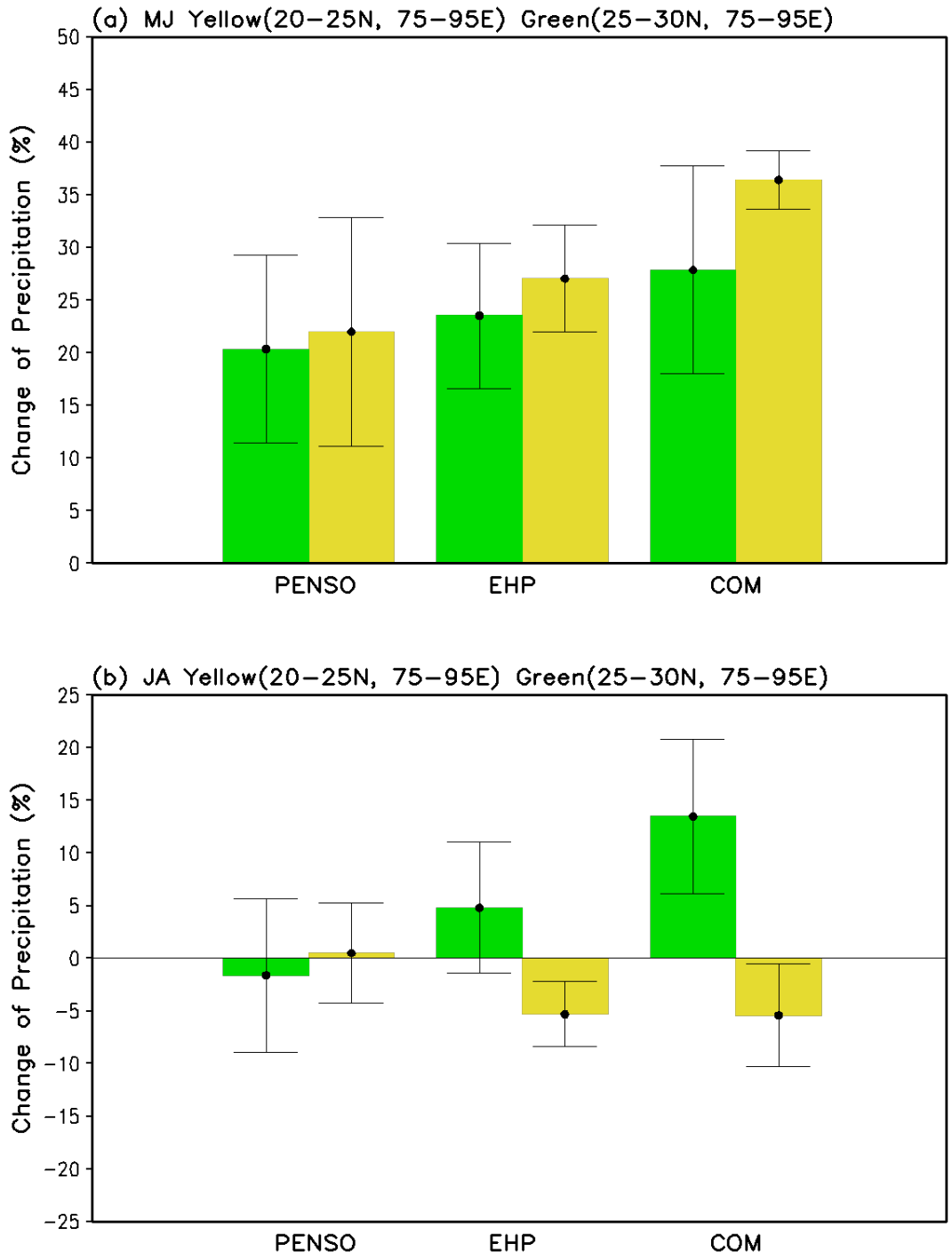

711

712 **Fig. 9** Changes in precipitation (color bars) induced by the PENSO, EHP, and combined (COM) effects
713 for (a) May-June and (b) July-Aug. Vertical Error line bars represent mean standard error of change in
714 precipitation. Green denotes the Himalayan foothills (25-30°N, 75-95°E); yellow denotes the Indo-
715 Gangetic Plain (20-25°N, 75-95°E)